Modeling first-order scattering processes from OSIRIS-REx color images of the rough surface of asteroid (101955) Bennu

Pedro H. Hasselmann[1], Sonia Fornasier[1,2], Maria A. Barucci[1], Alice Praet[1], Beth E. Clark[3], Jian-Yang Li[4], Dathon Golish[5], Daniella N. DellaGiustina[5], J. D. P. Deshapriya[1] , Xiao-Duan Zou[4] , Mike G. Daly[6] , Olivier S. Barnouin[7] , Amy A. Simon[8], Dante S. Lauretta[5] .

[1] LESIA, Observatoire de Paris, Université PSL, CNRS, Université de Paris, Sorbonne Université, 5 place Jules Janssen, 92195 Meudon, France.
[2]Institut Universitaire de France (IUF), 1 rue Descartes, 75231 Paris, France.
[3]Department of Physics and Astronomy, Ithaca College, Ithaca, NY, USA.
[4]Laboratory California Institute of Technology 21, Planetary Science Institute, Tucson, AZ, USA.
[5]Lunar and Planetary Laboratory, University of Arizona, Tucson, AZ, USA.
[6.] The Centre for Research in Earth and Space Science, York University, Toronto, Ontario, Canada.
[7.] The Johns Hopkins University Applied Physics Laboratory, Laurel, MD, USA.
[8.] NASA Goddard Space Flight Center, Greenbelt, MD, USA.

Introduction: The OSIRIS-REx mission has revealed a dark, boulder-rich, apparently dust-poor surface of the B-type asteroid (101955) Bennu [1], therefore a challenge for bi-directional reflectance (r_F) modeling. With an estimated geometric albedo of 4.5% [2], Bennu is darker than many comets, and its reflectance distribution is dominated by single-scattering processes.

The general approach to model a dark asteroid's bi-directional reflectance distribution is to apply the standard Hapke IMSA model and its shadowing function [3]. However, this can imprecisely describe the roughness slopes for rocky surfaces [4]. Assuming that surfaces are fully diffuse can negate a specular forward-scattering contribution from crystalline components in the regolith [7].

To achieve a more complete photometric modeling of Bennu's scattering curve, we rely on the radiative transfer semi-numerical model of Van Ginneken et al. [8]. It has successfully described the reflectance distribution for high reflectivity laboratory samples and the lunar phase curve [9].

Observations: MapCam is an optical imager [10] on-board the OSIRIS-REx spacecraft, equipped with four broadband color filters (60-90 nm wide) centered at 473 (b'), 550 (v'), 698 (w') and 847 (x') nm. We analyzed images acquired during the Equatorial Station (EQ), campaign of the Detailed Survey mission phase [11], over a full rotation of (101955) Bennu at a nadir spatial resolution of ~33 cm/px. EQ comprehended seven phase angle configurations α =[7.5° ,30° ,45° ,90° ,130°] .

We analyzed the pixel subtended by the mission's candidate sample collection sites, for which highly precise, laser altimeter-based digital terrain models (DTMs) were available [12,13]. These four candidate sites were called Sandpiper (latitude=-47°; longitude=322°), Osprey (11°; 88°), Nightingale (56°; 43°), and Kingfisher (11°; 56°). The varied latitude and longitudes provided the range of observational conditions required for our analysis.

Methodology: The methodology consists of the following steps:

a) NAIF SPICE kernels [14] and the DTMs are ingested into a ray-tracing code for rendering shadowed images. This allows us to discount for the effects of macroscopic shadows, leaving only the sub-facet texture to be modeled. These ancillary images provide the incidence, emergence, phase & azimuth for every facet.

b) We apply Van Ginneken's model to every facet. Occlusion and shadowing are taken into account by the model, as well as the retro-reflection among the reliefs. The model has two major components: the analytical expression for the specular reflection; and the numerically-integrated diffusive reflection. At total, the model has three free parameters: $\boldsymbol{\rho}$ (single-scattering albedo), $\boldsymbol{\sigma}$ (RMS roughness slope), and **g** (specular-to-diffuse ratio), plus the three more related to the scattering phase function (bi-lobe Henyey-Greenstein function: **c**, $\mathbf{b_1}$ and $\mathbf{b_2}$)

c) Inverse problem: We run the Monte Carlo Markov Chain (MCMC, pyMC 2.3) to sample the multi-parametric space in order to reconstruct a posteriori probability distribution of solutions for every free parameter, i.e., (ρ, σ, g, b1, b2, c),

from which the statistics for every solution are estimated.

In our implementation, we computed the chain jumps using the adaptive Metropolis-Hasting method. We dispatched a chain of 5000 steps. In the first run, as no previous information was available about any parameter, we considered *a priori* uniform probability distributions in the proper range defined for each parameter.

Results: The MCMC technique yields *a posteriori* parametric distributions for each parameter, revealing some interesting aspects of Bennu's surface (Fig. 1): while the RMS roughness slope of 27^{+1}_{-5} is in line with what has been obtained for other asteroids using Hapke shadowing function, we are puzzled by the indication of a non-zero specular reflection ratio from the surface ($2.6^{+1}_{-0.8}$ %). The specular reflection hints at possible mono-crystalline component.

As for the diffuse rough component, the meso-scale "rocky" topography contribution is pre-modeled through the use of DTM ray-tracing, leaving the micro-scale roughness to be described by the radiative model. However, the analysis of the photometric correction of OCAMS images taken at varied phase angles (α) indicates a more complex scenario. Up to $\alpha = 90°$, the photometric correction is vastly improved by mixing two different solutions for roughness (one with low RMS σ and another with global RMS σ), a bi-modality already perceived from the MCMC *a posteriori* distributions. We have shown that most of Bennu's brightness variation can be explained by tuning the roughness slope distribution.

Finally, we report a back-scatter phase function for the phase angle range between 7.5°, and 130°, without any expressive spectral trend in the visible range. The MCMC inversion hints at a possible second forward-scatter lobe of at least ~0.2 width. This leads to two possible solutions for the asymmetric factor ($\xi^{(1)} = -0.360 \pm 0.030$ and $\xi^{(2)} = -0.444 \pm 0.020$). We also report a dark global approximate single-scattering albedo at 550 nm from the collective analysis of all site candidates of $4.64^{+0.08}_{-0.09}$ % . The single-scattering MapCam four-band colors show a similar spectral trend to the global average OVIRS EQ3 spectrum. The four sites together provide a general description of Bennu's colors.

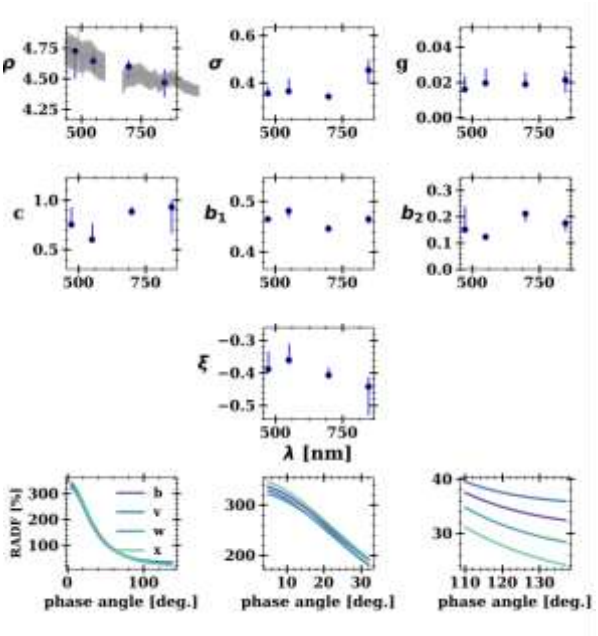

Fig. 1. Parametric solutions after the MCMC technique for all sample sites together, and the scattering phase function (bottom row) for each MapCam filters.

Acknowledgements: PHH, SF, MAB, AP, and JDPD acknowledge funding support by CNES. PHH acknowledges funding provided by Ile-de-France & Dim-ACAV+. This material is based upon work supported by NASA under Contract NNM10AA11C issued through the New Frontiers Program .The authors also extend their gratitude to the following people without whom this work would not have been possible: the instrument teams at NASA Goddard Spaceflight Center (GSFC) and Arizona State University; the spacecraft teams at GSFC, KinetX and Lockheed Martin; the science planning and operations teams at the University of Arizona; and the Science Processing and Operations Center staff at the University of Arizona.

References:

[1] Lauretta, D. et al. *Met.. & Plan. Scie.*, **50**, Issue 4, 834-849, 2015.

[2] DellaGiustina, D.N. et al., *Nat. Astron.* **3,** 241-351, 2019.

[3] Hapke, B. *Icarus* **59**, 41-59,1984.

[4] Shkuratov et al., *JQSRT* **113**, 18, 2431-2456, 2012.

[5] Davidsson, B. et al. *Icarus* **201,** 335–357, 2009.

[6] Labarre, S. et al. *Icarus* **290**, 63-80, 2017.

[7] Bowell, E., et al. *Asteroid* II, Univ. of Ariz. Press, 1989.

[8] Van Ginneken, B. et al. *Applied Optics,* **37**, 130-139, 1998.

[9] Goguen, J. et al. *Icarus* **208**, 548–557, 2010.

[10] Rizk, B. et al.. *Space Sci. Rev.* **214**, 26, 2018.

[11] DellaGiustina, D.N. et al., *ESS* **5**, 929, 2018.

[12] Daly, M. G. et al., *SSR* **212**, 899, 2017.

[13] Barnouin, O. S. et al., *PLANSS* **180**, 104764, 2020.

14] Acton, C. H.. *PLANSS* 44.1 (1996): 65-70.

[15] Hapke, B. Cambridge Univ. Press, 2nd ed., 2012.

Introduction: The OSIRIS-REx mission has revealed a dark, boulder-rich, apparently dust-poor surface of the B-type asteroid (101955) Bennu [1], therefore a challenge for bi-directional reflectance (r_F) modeling. With an estimated geometric albedo of 4.5% [2], Bennu is darker than many comets, and its reflectance distribution is dominated by single-scattering processes. The general approach to model a dark asteroid's bi-directional reflectance distribution is to apply the standard Hapke IMSA model and its shadowing function [3]. However, this can imprecisely describe the roughness slopes for rocky surfaces [4]. Assuming that surfaces are fully diffuse can negate a specular forward-scattering contribution from crystalline components in the regolith [7]. To achieve a more complete photometric modeling of Bennu's scattering curve, we rely on the radiative transfer semi-numerical model of Van Ginneken et al. [8,9].

Observations: MapCam is an optical imager [10] on-board the OSIRIS-REx spacecraft, equipped with four broadband color filters (60-90 nm wide) centered at 473 (b'), 550 (v'), 698 (w') and 847 (x') nm. We analyzed images acquired during the Equatorial Station (EQ), a campaign of the Detailed Survey mission phase [11], over a full rotation of (101955) Bennu at a nadir spatial resolution of ~33 cm/px. EQ comprehended seven phase angle configurations α =[7.5° ,30° ,45° ,90° ,130°] .

We analyzed the pixel subtended by the mission's candidate sample collection sites, for which highly precise, laser altimeter-based digital terrain models (DTMs) were available [12,13]. These four candidate sites were called Sandpiper (latitude=-47°; longitude=322°), Osprey (11°; 88°), Nightingale (56°; 43°), and Kingfisher (11°; 56°). The varied latitude and longitudes provided the range of observational conditions required for our analysis.

Methodology: The methodology consists of the following steps:

a) NAIF SPICE kernels [14] and the DTMs are ingested into a ray-tracing code for rendering shadowed images. This allows us to discount for the effects of macroscopic shadows, leaving only the sub-facet texture to be modeled. These ancillary images provide the incidence, emergence, phase & azimuth for every facet.

b) We apply Van Ginneken's model to every facet. Occlusion and shadowing as well as the retro-reflection among the reliefs are taken into account. The model has two major components: the analytical expression for the specular reflection; and the numerically-integrated diffusive reflection. At total, the model has three free parameters: **ρ** (single-scattering albedo), **σ** (RMS roughness slope), and **g** (specular-to-diffuse ratio), plus the three more related to the scattering phase function (bi-lobe Henyey-Greenstein function: **c**, $\mathbf{b_1}$, and $\mathbf{b_2}$)

c) Inverse problem: We run the Monte Carlo Markov Chain to sample the multi-parametric space in order to reconstruct a posteriori probability distribution of solutions for every free parameter, i.e., (ρ, σ, g, b1, b2, c), from which the statistics for every solution are estimated.

Results: The MCMC technique reveals some interesting aspects of Bennu's surface (Fig. 1): while the RMS roughness slope of 27^{+1}_{-5} is in line with what has been obtained for other asteroids using Hapke shadowing function, we are puzzled by the indication of a non-zero specular reflection ratio from the surface ($2.6^{+1}_{-0.8}$ %). The specular reflection hints at a possible mono-crystalline component.

As for the diffuse rough component, the analysis of the photometric correction of OCAMS images taken at varied phase angles (α) indicates a more complex scenario. Up to α = 90°, the photometric correction is vastly improved by mixing two different solutions for roughness (one with low RMS σ and another with global RMS σ), a bi-modality already perceived from the MCMC *a posteriori* distributions. We have shown that most of Bennu's brightness variation can be explained by tuning the roughness slope statistical distribution.

Finally, we report a back-scatter phase function for the phase angle range between 7.5°, and 130°, without any expressive spectral trend in the visible range. The MCMC inversion hints at a possible second forward-scatter lobe of at least ~0.2 width. This leads to two possible solutions for the asymmetric factor ($\xi^{(1)} = -0.360 \pm 0.030$ and $\xi^{(2)} = -0.444 \pm 0.020$). We also report a dark global approximate single-scattering albedo at 550 nm from the collective analysis of all site candidates of $4.64^{+0.08}_{-0.09}$ % . The single-scattering MapCam four-band colors show a similar spectral trend to the global average OVIRS EQ3 spectrum. The four sites together provide a general description of Bennu's colors.

Fig. 1. Parametric solutions after the MCMC technique for all sample sites together, and the scattering phase function (bottom row) for each MapCam filters.

References:

[1] Lauretta, D. et al. *Met.. & Plan. Scie.*, **50**, Issue 4, 834-849, 2015.

[2] DellaGiustina, D.N. et al., *Nat. Astron.* **3,** 241-351, 2019.

[3] Hapke, B. *Icarus* **59**, 41-59,1984.

[4] Shkuratov et al., *JQSRT* **113**, 18, 2431-2456, 2012.

[5] Davidsson, B. et al. *Icarus* **201,** 335–357, 2009.

[6] Labarre, S. et al. *Icarus* **290**, 63-80, 2017.

[7] Bowell, E., et al. *Asteroid* II, Univ. of Ariz. Press, 1989.

[8] Van Ginneken, B. et al. *AO* **37**, 130-139, 1998.

[9] Goguen, J. et al. *Icarus* **208**, 548–557, 2010.

[10] Rizk, B. et al.. *Space Sci. Rev.* **214**, 26, 2018.

[11] DellaGiustina, D.N. et al., *ESS* **5**, 929, 2018.

[12] Daly, M. G. et al., *SSR* **212**, 899, 2017.

[13] Barnouin, O. S. et al., *PLANSS* **180**, 104764, 2020.

[14] Acton, C. H.. *PLANSS* **44.1** (1996): 65-70.

[15] Hapke, B. Cambridge Univ. Press, 2ed., 2012.